Measuring peroxidasin activity in live cells using bromide addition for signal amplification

Veronika F.S. Pape [a],[**], Hajnal A. Kovács [a], István Szatmári [b], Imre Ugrai [b], Bence Szikora [c], Imre Kacskovics [c], Zoltán May [d], Norbert Szoboszlai [e], Gábor Sirokmány [a], Miklós Geiszt [a],[*]

[a] *Department of Physiology, Semmelweis University, Faculty of Medicine, Tűzoltó utca 37-47, H-1094, Budapest, Hungary*
[b] *Institute of Pharmaceutical Chemistry and Stereochemistry Research Group of Hungarian Academy of Sciences, University of Szeged, Eötvös u. 6, H-6720, Szeged, Hungary*
[c] *ImmunoGenes Ltd., Budakeszi, Hungary*
[d] *Research Centre for Natural Sciences, Eötvös Loránd Research Network, Magyar Tudósok körútja 2, H-1117, Budapest, Hungary*
[e] *Institute of Chemistry, Eötvös Loránd University, Pázmány Péter sétány 1/A, H-1117, Budapest, Hungary*

ARTICLE INFO

ABSTRACT

Peroxidasin (PXDN) is involved in the crosslinking of collagen IV, a major constituent of basement membranes. Disruption of basement membrane integrity as observed in genetic alterations of collagen IV or PXDN can result in developmental defects and diverse pathologies. Hence, the study of PXDN activity in (patho)physiological contexts is highly relevant. So far, measurements of PXDN activity have been reported from purified proteins, cell lysates and de-cellularized extracellular matrix. Here, for the first time we report the measurement of PXDN activity in live cells using the Amplex Red assay with a signal amplifying modification. We observe that bromide addition enhances the obtained signal, most likely due to formation of HOBr. Abrogation of signal amplification by the HOBr scavenger carnosine supports this hypothesis. Both, pharmacological inhibition as well as complementary genetic approaches confirm that the obtained signal is indeed related to PXDN activity. We validate the modified assay by investigating the effect of Brefeldin A, to inhibit the secretory pathway and thus the access of PXDN to the extracellular Amplex Red dye. Our method opens up new possibilities to investigate the activity of PXDN in (patho)physiological contexts.

1. Introduction

Members of the peroxidase-cyclooxygenase superfamily mediate diverse effects of hydrogen peroxide in living organisms. In mammals, myeloperoxidase (MPO) eosinophil peroxidase (EPO) and lactoperoxidase (LPO) serve in host defense through the formation of oxidized halides and pseudohalides [1,2]. Similarly, the enzyme thyroid peroxidase (TPO) oxidizes iodide into reactive derivatives, which play a crucial role in the synthesis of thyroid hormones [1,2]. A role for peroxidases in the synthesis and modification of the extracellular matrix (ECM) has been known for a while, but these reactions were initially thought to be restricted to lower organisms [3]. The discovery of peroxidasin (PXDN) in *Drosophila melanogaster* suggested that a link between the extracellular matrix formation and reactive oxygen species can reside in the form of a heme-containing peroxidase [4,5].

The ECM, consisting of interstitial matrix and basement membrane, provides structural support for cells, but also mediates response to mechanical and chemical stimuli [6,7]. Cellular interactions with the ECM are important in order to maintain and regulate cellular function, e.g. in tissue development, maintenance and in response to injury [6,7]. The sheet-like structures of the basement membrane underlie epithelia and endothelia, surround muscle cells, peripheral nerves and adipose tissue

[6,8]. A major constituent of the basement membrane is collagen IV [6–8].

Genetic alterations in collagen IV isoforms are associated with disease development such as Alport syndrome, nephritic syndrome (hematuria and proteinuria), porencephaly (degenerative brain cavities in newborn infants), and the development of hemorrhages [7].

While other enzymes also cross-link other collagen isoforms, PXDN is selective for collagen IV, and to our current knowledge, collagen IV is the primary target of this peroxidase [9]. The presence of the PXDN gene is ubiquitous in animals and the enzyme plays a central role in the formation of basement membranes through the crosslinking of collagen IV protomers [6,8]. The covalent cross-linking between the NC1 domains of collagen IV occurs via formation of a bromosulfonium cation at methionine 93, facilitating the reaction with opposing lysine/hydroxylysine 211. The reactive bromosulfonium intermediate is obtained following oxidation by PXDN-produced hypobromous acid (HOBr) [9,10]. The resulting sulfilimine bond, first described in collagen IV synthesis in living organisms, helps stabilize the collagen IV network that forms the basis of basement membranes [6,8,11]. Although HOBr is a highly reactive and potentially damaging compound, PXDN-mediated oxidative protein crosslinking is a physiological process of mammalian tissue genesis [6,8]. In PXDN-KO mice NC1 domains of collagen IV are not covalently cross-linked, resulting in reduction in tissue stiffness [12]. Furthermore, the fundamental role of the PXDN-catalyzed reaction is well illustrated by a severe ocular phenotype of PXDN deficiency in both mice and humans [13].

A unique feature of the enzymatic action of PXDN is that it shows high selectivity for bromide and cannot oxidize chloride, which is a much more abundant anion in the organism [6,14]. This selectivity is important because it prevents the formation of hypochlorous acid (HOCl) which would probably exert harm on the PXDN-expressing and surrounding cells. Nevertheless, the target of hypobromous acid is probably not restricted to well-defined regions of collagen IV, as tyrosine residues were also described to be oxidized by HOBr, resulting in the formation of brominated tyrosine rings [15,16]. The physiological significance of the latter reaction is so far unclear, and the identity of the proteins modified by this mechanism is also awaiting identification. However, it is possible that under some conditions and/or in specific tissues, PXDN-mediated bromination does represent a physiologically important mechanism of protein modification.

The enzymatic activity of PXDN is often tested by the analysis of the crosslinking state of NC1 domains following the collagenase-mediated digestion of cell culture lysates [11]. Peroxidase assays were also reported to measure the activity of the purified enzyme or PXDN activity in cell lysates and decellularized ECM [4,17–20]. We observe a signal amplification in the Amplex Red assay in the presence of increasing bromide concentrations that enables for the first time the measurement of PXDN activity in live cells. Presumably this amplification is due to a direct oxidation of Amplex Red by HOBr, which is formed by PXDN from bromide and hydrogen peroxide. Multiple lines of genetic evidence support the conclusion that the observed (enhanced) oxidation of Amplex Red is mediated by PXDN. This signal amplification method offers a valuable tool to study the PXDN activity of primary and cancerous cell cultures and to investigate PXDN activity in physiological contexts. As an example, we show that this method enables us to follow the effect of Brefeldin A (BFA) on the dynamics of PXDN trafficking and secretion in live cells.

2. Material and methods

2.1. Cell culture

HEK-293-T cells (ATCC, Manassas, VA, USA, CRL-3216), PFHR-9 cells (ATCC, Manassas, VA, USA, CRL-2423) and PXDN-KO PFHR-9 cells (prepared by Cas9 CrispR method in our laboratory earlier [21]) as well as Resc-wt and Resc-mut cells were grown in Dulbecco's Modified Eagles Medium with glutamine and 4,5 g/L glucose, supplemented with 10% fetal bovine serum (Lonza Group Ltd., Basel, Switzerland), 50 U/mL penicillin and 50 μg/mL streptomycin (Lonza Group Ltd., Basel, Switzerland) in a humidified incubator with 5% CO_2 at 37 °C.

PFHR-9-Resc-wt and PFHR-9-Resc-mut cells were prepared from PXDN-KO PFHR-9 cells by transfection with the sleeping beauty transposon system [22]. Briefly, N-terminally Flag tagged WT PXDN (Resc-wt), or N-terminally Flag tagged and C-terminally V5 tagged Q823W and D826E mutant PXDN (Resc-mut) were cloned into a pSB-puro vector for transfection. Transfected cells were selected for puromycin and kept under selection (1.25 μg/mL puromycin) until one to five passages prior to experiments.

HCSMC (Lonza Group Ltd., Basel, Switzerland) and HAoSMC (kind gift of András Balla) were grown in smooth muscle cell basal medium 2 (PromoCell, Germany), supplemented with 5% fetal calf serum, 5 μg/mL insulin, 2 ng/mL hbFGF, 0.5 ng/mL hEGF (PromoCell, Germany), as well as 50 U/mL penicillin and 50 μg/mL streptomycin (Lonza Group Ltd., Basel, Switzerland).

2.2. Transfection of PFHR-9 cells with siRNA

Cells were seeded to a 96 well plate in a density of 10.000 cells/well (c/w) and let grow to approximately 70% confluency in antibiotics-free DMEM (supplemented with 10% FBS as above). Subsequently, cells were transfected with 40 nM of siRNA (either scrambled (#2, Thermo Scientific) or murine PXDN targeting (Thermo Scientific) with lipofectamine RNAiMax (invitrogen) for 48h prior to the experiment.

After the functional assay, supernatants were removed, and cells were lysed with 20 μL RIPA buffer (150 mM NaCl, 25 mM Tris, 0.1% SDS, 0.5% sodium deoxycholate, 1% Triton X100, pH 8, supplemented with HALT protease inhibitor cocktail (Thermo Scientific)) per well. Samples were scratched, supplemented with 7 μL 4x reducing Laemmli buffer per well, pooled and boiled for 5 min at 95 °C before applying them to gel electrophoresis and western blotting.

2.3. Antibodies

For the detection of PXDN in PFHR-9 cells, we developed a monoclonal antibody, adapting a previously described protocol [23]. A detailed description of the immunization and antibody production is provided in the supporting information.

For detection of PXDN in human SMCs we used a polyclonal PXDN specific antibody, previously developed in rabbit [17]. Primary antibodies used for western blots were purchased from Sigma Aldrich for detection of Flag-tag (mouse monoclonal Anti-FLAG M2 antibody, F3165), smooth muscle actin (mouse monoclonal antibody, A5228), and β-actin (mouse monoclonal antibody, A1978). HRP-conjugated secondary antibodies used for western blots, donkey anti-rabbit IgG (31458) and goat-*anti*-mouse IgG (31432), respectively, were purchased from Invitrogen.

2.4. Immunostaining of PXDN

Cells were seeded to black chimney clear bottom 96 well plates (Greiner 655090) at a density of 5.000 c/w and allowed to grow for 60 h prior to treatment with or without 5 μM Brefeldin A (Thermo Scientific, Hungary) for 12 h. Following treatment, cells were fixed with 4% paraformaldehyde in PBS for 45 min at room temperature and washed twice with 100 mM glycine containing PBS. For antigen retrieval, hot citrate buffer (10 mM, 0.1% Triton X-100) was applied for 5 min. Subsequently, samples were washed twice with PBS and blocked with 3% BSA containing PBS for 1 h. Samples were incubated with the hybridoma supernatant (diluted with 3% BSA in a ratio of 2:1, to achieve a final BSA concentration of 1%) overnight. After washing with PBS (6 times), the secondary antibody (Alexa Fluor 488 conjugated donkey anti-mouse IgG (A-21202, Thermo Scientific)) was applied in 1% BSA containing PBS,

together with 0.1 μM Hoechst 33342 for nuclear staining, for 1 h in the dark. Samples were washed with PBS (6 times) prior to imaging. Fluorescence signals were recorded with the ImageXpress Micro XL (Molecular Devices, Sunnyvale, CA, USA) high content screening system using a Nikon 40x objective.

2.5. Amplex Red assay on cell lysates

Cells were harvested and washed with H-medium (145 mM NaCl, 5 mM KCl, 1 mM MgCl$_2$, 0.8 mM CaCl$_2$, 5 mM Glc, 10 mM HEPES) twice, then counted and adjusted to a density of 100.000 cells in 65 μL. Subsequently, 65 μL of the cell suspension were plated per well to a 96 well plate (CytoOne or Greiner) and lysed with 5 μL of 20% (w/v) detergent CTAB (sigma) or CTAC (sigma) respectively. Following a 10 min incubation time, 10 μL of 10x concentrated Amplex Red (Synchem, Germany) solution was added (to achieve a final concentration of 50 μM) and the baseline fluorescence was measured using either a Clariostar (excitation: 577 nm, emission: 613 nm) or Polarstar (excitation: 580 nm, emission: 610 nm) plate reader (BMG, Germany). Subsequently, 10 μL of 10x concentrated bromide in H-medium was added and fluorescence was recorded for approximately 5 min, before 10 μL of 10x concentrated H$_2$O$_2$ was added in the indicated concentrations. The signal was followed for at least 60 more minutes. The slope over the initial 10 min upon addition of H$_2$O$_2$ was fitted separately for each replicate and used as an indicator for PXDN activity. In cases, where analysis was hampered by an unfavorable signal-to-noise ratio, areas under the curves were calculated, setting the measurement points prior to H$_2$O$_2$ addition as the baseline using GraphPad Prism [24].

2.6. Amplex Red assay on intact cells

Cells were harvested, counted, seeded to 96 well plates (CytoOne or greiner) in a cell density of 50.000 cells/well (unless stated otherwise) and let allow to grow for 72h. Before the assay, they were washed with H-medium, layered with 70 μL H-medium and baseline fluorescence was measured upon addition of 10 μL of 10x concentrated Amplex Red (Synchem, Germany) solution (to achieve a final concentration of 50 μM, unless stated otherwise) using either a Clariostar (excitation: 577 nm, emission: 613 nm) or Polarstar (excitation: 580 nm, emission: 610 nm) plate reader (BMG, Germany). Subsequently, 10 μL of 10x concentrated bromide in H-medium was added and fluorescence was recorded for approximately 5 min, before 10 μL of 10x concentrated H$_2$O$_2$ was added in the indicated concentrations. The signal was followed for at least 60 more minutes. The slope over the initial 10 min upon addition of H$_2$O$_2$ was fitted separately for each replicate and used as an indicator for PXDN activity. In cases, where analysis was hampered by an unfavorable signal-to-noise ratio, areas under the curves were calculated separately for each replicate, setting the measurement points prior to H$_2$O$_2$ addition as the baseline using GraphPad Prism [24].

2.7. Preparation of decellularized extracellular matrix

PFHR-9 WT and PXDN-KO cells were grown to overconfluency (for 96 well plates 50.000 cells, for 24 well plates 0.3 Mio cells were seeded per well 72h prior to 6–12h treatment with Brefeldin A. The ECM was decellularized using a well-established hypotonic washing protocol [25]. Briefly, cells were gently washed twice with hypotonic buffer (5 mM Tris-HCl, 0.5 mg/mL BSA, 0.1 mM CaCl$_2$, pH 7.5), followed by a 10 min incubation in the same buffer at 37 °C and two 1 min long extractions at 37 °C using the hypotonic buffer supplemented with 0.5% Nonidet P-40. The thus obtained cell-free matrices were washed 5x with H-medium and subjected to subsequent measurements of PXDN activity with Amplex Red assay.

2.8. Reagents

H$_2$O$_2$, NaBr, carnosine, and NAC were obtained from Sigma Aldrich (Hungary), reagents for preparation of bromine free salts were obtained from Molar Chemicals (Hungary) and used without further purification. HOCl was obtained from Hip-Tom (Hungary).

2.9. Preparation of bromine free NaCl and KCl

Bromine free salts were prepared applying a slightly modified protocol of McCall et al. [10,26], providing NaCl in an overall yield of 68.4% and KCl in a yield of 56.8%. A detailed description of the protocol is provided in the supporting information.

2.10. Analysis of bromine content with ICP-MS

We used inductively coupled plasma mass spectrometry (ICP-MS) to determine the bromine content of commercial and synthesized salts. To this end, the 50 mg of the sample salts were dissolved in 5 mL ultrapure water (ELGA, 18.2 MΩ/cm). These sample solutions were measured with Thermo Fisher Scientific iCAP Q quadrupole ICP-MS in KED mode (Kinetic Energy Discrimination, applying high purity helium gas). For quantitative analysis, an external calibration was performed, using sodium bromide salt (Sigma-Aldrich) in 50, 100 and 1000 μg/L concentrations.

2.11. Analysis of bromine content with TXRF

For the total-reflection X-ray fluorescence (TXRF) analysis, 100 μL of H-medium prepared from commercial salts or synthesized salts, respectively, were mixed with 20 μL of 30% H$_2$O$_2$ and 80 μL of 65% HNO$_3$. To that solution, 20 μL of 15 μg/mL Ga(NO$_3$)$_3$ (in nitric acid) was added as an internal standard. From the resulting solutions, 2 μL were pipetted on the quartz reflectors. Measurements were performed on an Atomika 8030C TXRF spectrometer (Atomika Instruments GmbH, Oberschleissheim, Germany). The Kα line used for determination of Br was at 11.924 keV.

2.12. Preparation of HOBr

HOBr was prepared as reported earlier [27,28]. Briefly, the concentration of HOCl was determined from absorbance values measured at 292 nm using UV transparent 96 well plates (Greiner 655801) and a Clariostar pate reader (BMG, Germany) and adjusted to 100 mM. The adjusted HOCl was mixed with 1.2 equivalents of NaBr from a 1 M stock solution and mixed by vortexing for 5 min. Subsequently, the concentration of HOBr was determined from absorbance values measured at 332 nm. No HOCl traces were visible in the absorbance spectra of HOBr (see Figure S5).

3. Results

3.1. Amplex Red oxidation by peroxidasin is enhanced in the presence of bromide in cell lysates

The murine embryonic cancer cell line PFHR-9 expresses and secretes high amounts of PXDN, and hence serves as a good model to study PXDN activity. As a control, we additionally used PFHR-9 cells, where the PXDN gene was disrupted by the CRISPR/Cas9 technique (PXDN KO cells) [21].

The measurement of PXDN activity from purified proteins, cell lysates and decellularized extracellular matrix is feasible with diverse peroxidase assays, including the Amplex Red assay.

In this assay, the non-fluorescent (Amplex Red) substrate is oxidized to fluorescent resorufin by a peroxidase in the presence of H$_2$O$_2$ [29]. This assay has been frequently employed to measure PXDN activity in

lysates prepared with the detergent cetrimonium bromide (CTAB, Hexadecyltrimethylammonium bromide), that is supposed to inhibit nonspecific oxidations catalyzed by heme (proteins) [4,17–19].

In Fig. 1, we show the activity of PXDN in CTAB lysates of PFHR-9 WT (Fig. 1A) and PXDN-KO PFHR-9 (Fig. 1B) cells in an H_2O_2 dependent manner. The rate of Amplex Red oxidation was quantified by fitting the slope of signal increase over the first 10 min following addition of H_2O_2 (Fig. 1C). Since bromide is the counter anion in the cationic detergent CTAB, application of 1% (w/v) of this detergent in the lysis buffer corresponds to a bromide concentration of as high as 27.4 mM. To investigate, whether bromide had an impact on the observed signal, we changed the counter anion in the detergent and used cetrimonium chloride (CTAC) instead. Interestingly, this anion change completely abrogated fluorescence observed in the functional assay (Fig. 1D, grey dots). However, the lost activity could be restored by addition of bromide in a concentration-dependent manner (see colored curves in Fig. 1D). Restoration of the signal was diminished by the peroxidase inhibitor phloroglucinol (PHG) in a dose dependent manner (Figure S1), and could not be achieved in lysates of PXDN-KO PFHR-9 cells (Fig. 1E), suggesting that indeed PXDN is responsible for the observed effect.

3.2. Effect of bromide on Amplex Red oxidation in intact cells

Encouraged by the observed enhancement of fluorescence by bromide supplementation of the reaction buffer, we wanted to know, if we could apply the same approach to measure PXDN activity in intact cells. Indeed, we could successfully measure the enzymatic activity of PXDN in live cells (Fig. 2). Cells were seeded 72h prior to the experiment and reached overconfluency at the day of measurement. Addition of bromide enhances the signal in Amplex Red assay performed on intact PFHR-9 WT cells (Fig. 2A) up to 3.4 times. As observed for the lysates, also on intact cells, co-administration of PHG completely abrogated Amplex Red oxidation (Figure S2) at as low concentrations as 0.1 μM. Furthermore, bromide addition had no effect on the signal in PFHR-9 PXDN-KO cells (Fig. 2B), again confirming a role of PXDN in the bromide amplified oxidation of Amplex Red. Compared to the experiments performed in lysates (Fig. 1), the Amplex Red oxidation rate increases with a less steep slope, but overall reaches higher values. Furthermore, a dependence on

both H_2O_2 (Fig. 2C and D) and bromide (Fig. 2E and F) concentrations is clearly visible.

3.3. Is oxidation of Amplex Red possible in the absence of bromide?

As evident from Fig. 2A, even in the absence of bromide, PXDN-activity was measurable from intact PFHR-9 WT cells.

McCall et al. have shown, that trace amounts of bromide present in commercial salts result in significant bromide concentrations (around 6 μM) that are sufficient to catalyze crosslinking of collagen IV fibers [10]. Hence, we were wondering, if the observed activity without addition of extra bromide might be due to traces of bromide found in commercial salts.

Following the approach of McCall et al., we produced bromide-free NaCl and KCl by reacting sodium hydroxide with gaseous hydrogen chloride and prepared bromide free assay buffer from these salts [10]. ICP/MS (Table 1) as well as TXRF (not shown) measurements confirmed the absence of bromide in the synthesized salts, while showing significant amounts of bromide in the commercial salts, and buffers prepared from those (Table 1).

PXDN activity of PFHR-9 WT cells is still measurable in the absence of bromide (Fig. 2G,H). Inhibition of PXDN by PHG (1 μM) abrogates Amplex Red oxidation to resorufin. While in the presence of PHG, bromide had no effect on fluorescence, in the absence of the PXDN inhibitor, an increase in resorufin fluorescence is observed starting from bromide concentrations around 250 μM (Fig. 2H). Of note, addition of small bromide concentrations (below 100 μM) provokes a slight decrease in resorufin fluorescence (Fig. 2H).

3.4. Additional genetic evidence that PXDN is responsible for observed signal amplification in PFHR-9 cells

PXDN-KO PFHR-9 cells (lysed or intact), showed no oxidation of Amplex Red, and bromide addition did not have any effect on the observed signal (Fig. 2B,D,F).

In order to exclude the possibility that the lack of measurable peroxidase activity in KO cells was due to clonal selection, we knocked down PXDN transiently using siRNA (Fig. 3). Indeed, siRNA targeting
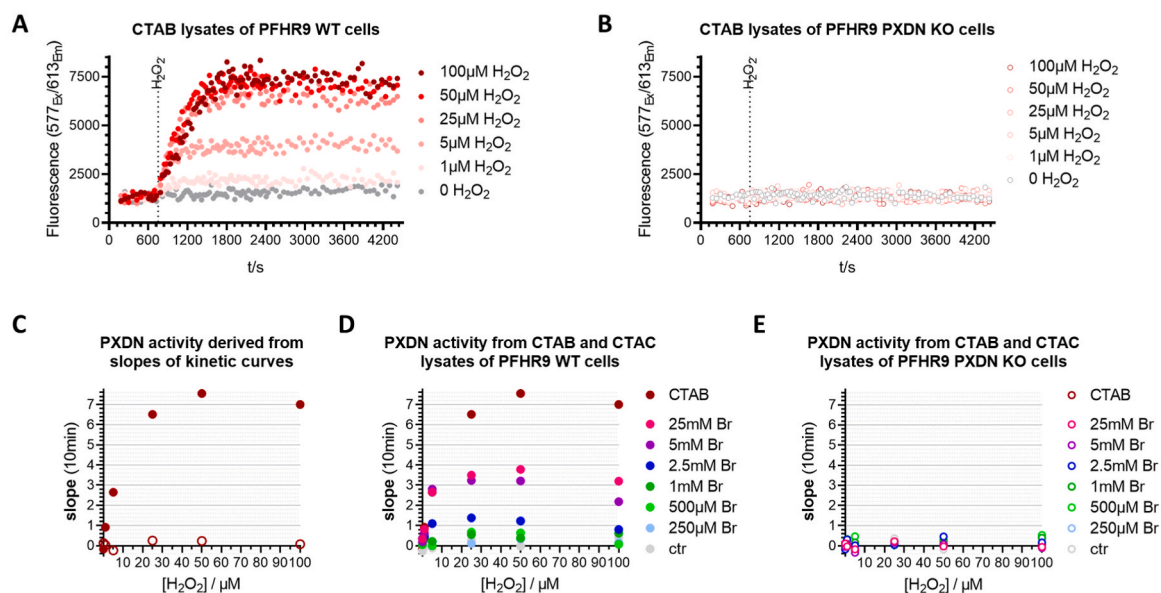

Fig. 1. Amplex Red fluorescence obtained with CTAB lysates of WT (A) and PXDN-KO (B) PFHR-9 cells with increasing concentrations of H_2O_2 (indicated by increasing intensity of red color). The slope of the kinetic curves for the first 10 min following H_2O_2 addition was analyzed for the measurements of panels A and B (C). Changing the detergent from CTAB to CTAC abolished the signal completely (D,E; grey dots, labeled as ctr), while supplementation of bromide to CTAC lysates from WT (D), but not from PXDN-KO cells (E), was able to restore the fluorescent signal. Data show results of a representative experiment out of four. (For interpretation of the references to color in this figure legend, the reader is referred to the Web version of this article.)
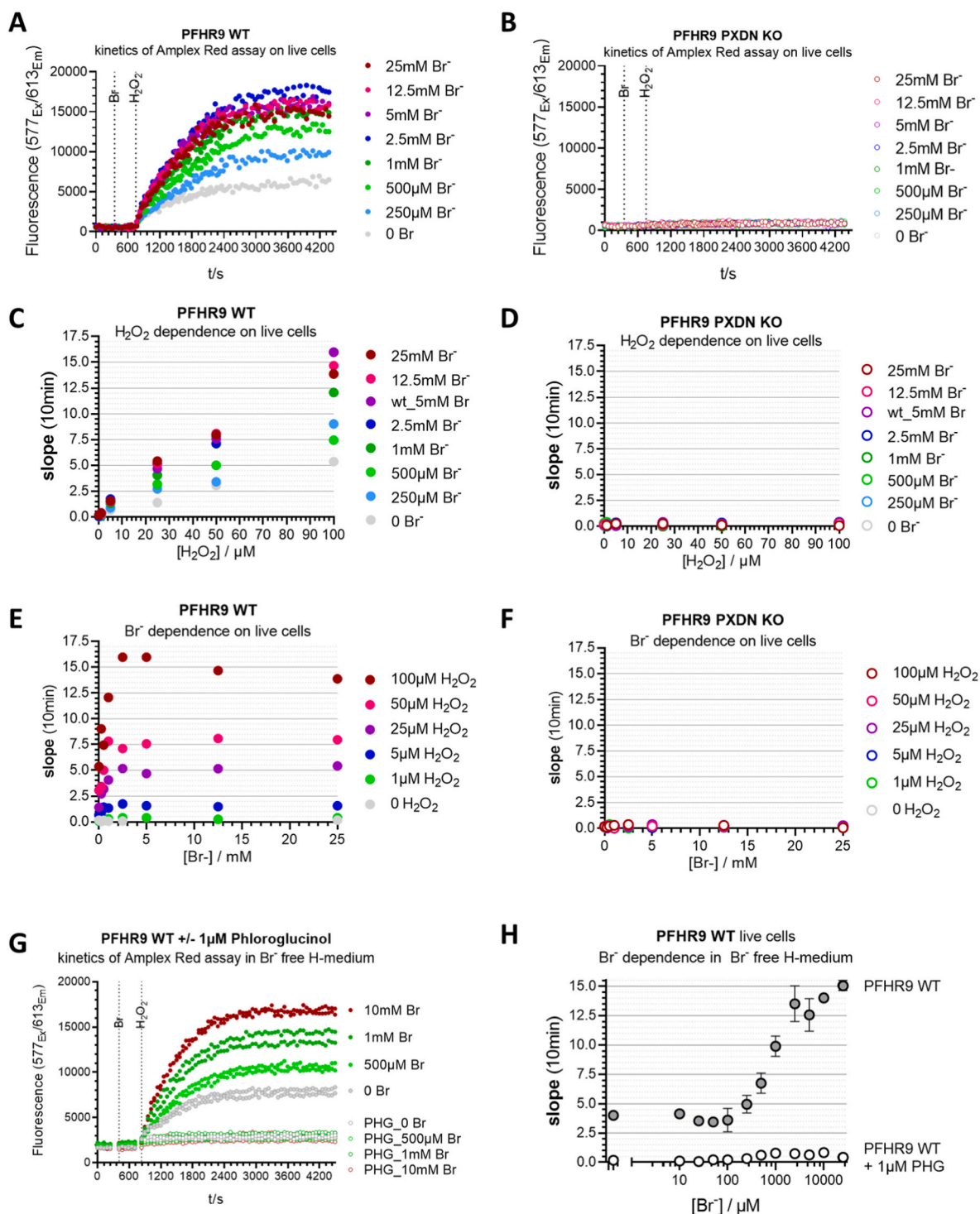
Fig. 2. Bromide enhances the signal in Amplex Red assay performed on intact PFHR-9 WT (A,C,E) cells, while leaving the signal in PFHR-9 PXDN-KO cells (B,D,F) unaffected. Time courses (A,B) and slope evaluation of the first 10 min following H_2O_2 addition are shown in dependence of H_2O_2 (C,D) and bromide (E,F) concentrations. Presented data show results of a representative experiment out of three. PXDN activity is still measurable in intact PFHR-9 WT cells, when the assay is performed in bromide-free H-medium in the absence (filled) and presence (open symbols) of 1 μM PHG (G,H). Cells were washed twice for 5 min with bromide-free H-medium prior to the measurements. For clarity, kinetics in panel G are shown only in the presence of four concentrations of bromide, exemplarily, while the slope analysis over the first 10 min after following addition of 50 μM H_2O_2 is shown for the full range of applied bromide concentrions (H). Results shown in panels G and H display results of a representative experiment out of 10, performed in duplicates. Cells were seeded in a density of 50.000 c/w 72h prior to measurement. (For interpretation of the references to color in this figure legend, the reader is referred to the Web version of this article.)

murine PXDN, largely diminished the observed activity as well as the bromide enhancing effect, almost down to the levels of KO cells, while scrambled siRNA had no inhibitory effect (Fig. 3C and D). The knock down of PXDN was confirmed on protein level by western blot (Fig. 3E),

using a newly developed monoclonal antibody.

As a next step, we set out to rescue the PXDN-KO phenotype by re-introducing PXDN to the PXDN-deficient cells. We created cell lines with the Flag-tagged wild-type protein (Resc-wt), as well as with a

Table 1

Bromide content was determined for commercial and synthesized salts used in assay buffer (H-medium) using ICP-MS. Contamination of bromide in commercial salts is given in ppm (mg/kg). Bromide traces in synthesized salts are at the border of the detection limit of the method.

Salt	Bromide/ ppm	Concentration in H-medium	Corresponds to Bromide in H-medium
Commercial NaCl	63.1	145 mM	5.197 µM
Synthesized NaCl	<0.25		<20.6 nM
Commercial KCl	46.9	5 mM	0.170 µM
Synthesized KCl	<0.25		<0.9 nM

Q823W, D826E mutation, destroying the peroxidase activity of the introduced enzyme (Resc-mut) [13,18].

As shown in Fig. 3F, Resc-wt and Resc-mut transfected PFHR-9-PXDN-KO cells express PXDN, detected by both Flag as well as PXDN antibodies. Of note, the PFHR-9 cell line is hard to transfect. Thus, it is apparent from the western blot developed against PXDN, that the re-introduction of PXDN did not reach the same expression levels as observed for the WT cells. Both, blots developed against Flag and PXDN indicate that the non-functional peroxidase mutant Resc-mut is expressed in higher levels as compared to the re-introduced wild-type protein in Resc-wt cells.

To characterize these cells, in a first step, we investigated the bromide and H_2O_2 dose dependent effect on CTAB (Fig. 3G) and CTAC lysates (Figure S4 A,B). Introduction of the full length protein was able to restore only a fraction of the activity observed in WT cells (Fig. 3G). However, taking into account the expression levels seen in western blots
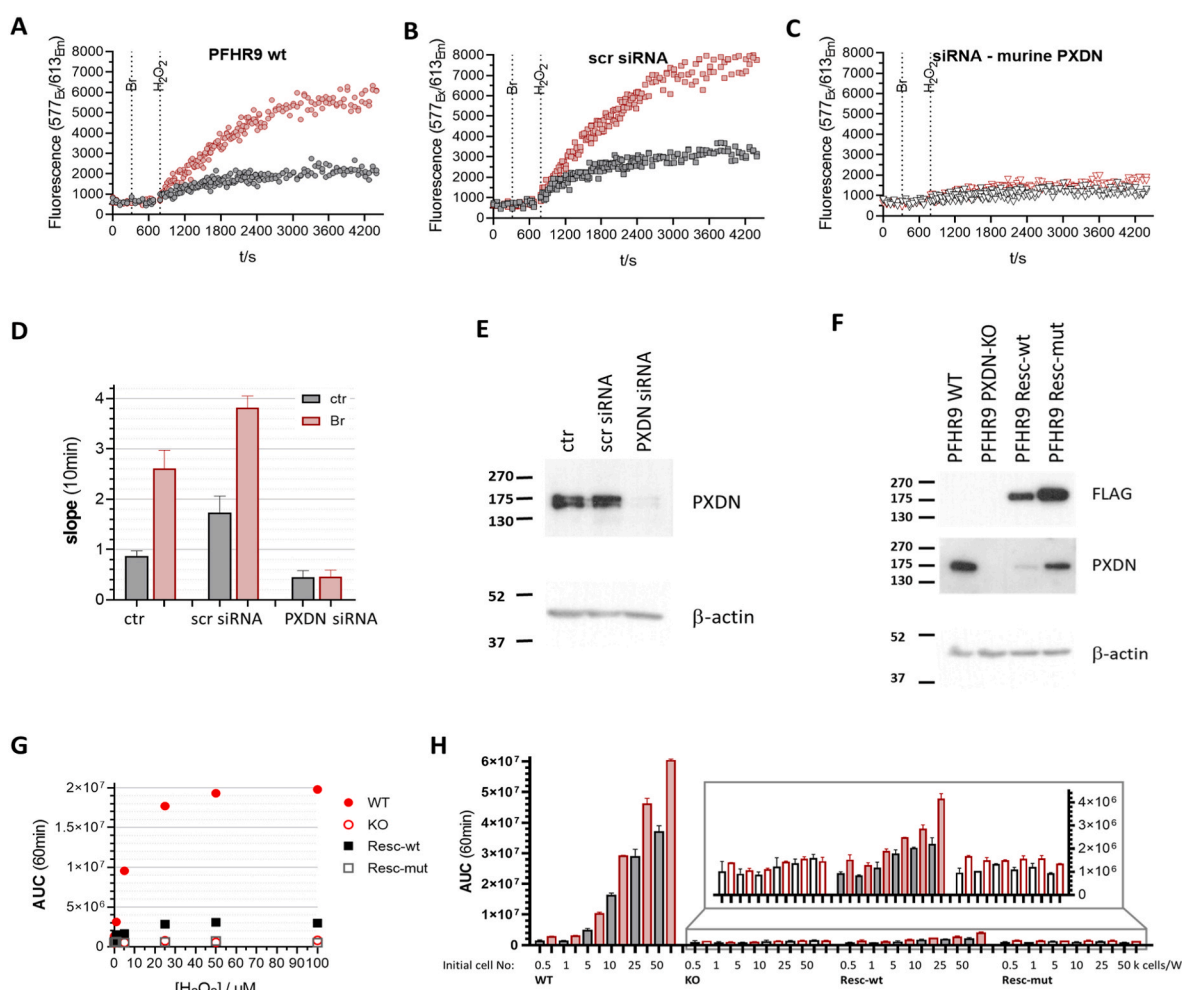

Fig. 3. Transient knock-down of PXDN, as well as rescue of signal by re-introduction of PXDN, but not of its non-functional mutant, confirm the involvement of PXDN in the observed signal amplification by bromide. Amplex Red assay measured on intact PFHR-9 cells (10.000 c/w seeded before transfection without siRNA (A), with scrambled siRNA (B), and with siRNA targeting the murine PXDN (C). For each panel, control conditions are shown in grey, enhanced PXDN activity by bromide addition (2.5 mM) is shown in bordeaux. Each line represents one out of two experiments performed in duplicates. Slopes, representing the Amplex Red oxidation rate are shown in panel D, following the same color code. Transient knock-down of PXDN was confirmed by western blot (E). PXDN was re-introduced to PFHR-9 PXDN KO cells using the sleeping beauty system. Protein expression of PXDN in PFHR-9 WT, PXDN-KO and Resc-wt, Resc-mut PFHR-9 cell lines is shown by western blot (F). Given the lower expression of PXDN in the rescue cell lines, as compared to the WT cells, analysis of the functional assays performed with these cell lines is shown as integrated area under the curves of a 60 min time course Amplex Red assay performed on CTAB lysates with PFHR-9 WT (red filled circles), PXDN-KO (red open circles), as well as PFHR-9-Resc-wt (black filled squares) and Resc-mut (black open squares) cells with increasing concentration of H_2O_2 (G). Both signals in the absence (grey) of bromide, and amplification in the presence of 2.5 mM bromide (bordeaux) increase with increasing cell number (H). PFHR9-WT, PXDN-KO, as well as Resc-wt and Resc-mut cells were seeded in the indicated densities 72h prior to the measurement. AUCs were calculated over 60min. Results show a representative experiment out of three to seven. (For interpretation of the references to color in this figure legend, the reader is referred to the Web version of this article.)

(Fig. 3F), one should not expect a full restoration of activity. Of note, the lower signal as compared to the PFHR-9 WT cells hampered a reliable analysis fitting slopes. Therefore, areas under the respective curves were calculated and are displayed in Fig. 3. For comparison, the analysis using the area under the curves for data presented in Figs. 1 and 2 are shown in Figure S3. As for the PFHR-9 WT cells, also for the Resc-wt cell line, expressing the full length protein, a bromide enhancing effect of fluorescence in the CTAC lysates (Figure S4A) and in intact cells (Figure S4C, E) could be observed, but not in the peroxidase-mutant expressing cell line Resc-mut (Figure S4D,F).

In line with the correlation of observed activity in Resc-wt cells with the lower expression as compared to the PFHR-9-WT cells, we observed a cell number-dependent increase in signal for PFHR-9-WT and Resc-wt cells, further confirming the dependence on the magnitude of observed signal on PXDN protein levels (Fig. 3H).

3.5. Possible involvement of HOBr in signal enhancement by bromide

Mammalian heme peroxidases can operate by two catalytic cycles: Once the heme center is oxidized by H_2O_2 to an oxy-ferryl form (compound I) and a porphyrin-cation radical, the ferric enzyme can be restored either by the so called "halogenation cycle", representing a two-electron reduction by halides or pseudo-halides, or via the "peroxidase cycle", consisting of two sequential one-electron reduction steps, thereby oxidizing organic substrates [1].

In the Amplex Red assay, the non-fluorescent dye is oxidized to fluorescent resorufin in the "peroxidase cycle" of the enzyme [1,30]. Given that Amplex Red might be directly oxidized by HOCl [31], we were wondering if the signal amplifying effect of bromide addition might be due to a direct oxidation of the dye by HOBr produced in the "halogenation cycle" of PXDN.

Therefore, we first investigated the chemical oxidation of Amplex Red to resorufin by HOBr, which we prepared chemically by oxidizing NaBr with HOCl [27,28] (Figure S5). Indeed, as for HOCl, we also observed oxidation of Amplex Red by HOBr (Fig. 4A and B). Note-worthy, oxidation of Amplex Red by HOBr (Fig. 4A) appears to happen much faster as compared to its oxidation by HOCl (Fig. 4B).

In a next step, we aimed to scavenge HOBr, in order to reveal the part of amplification, that could be related to HOBr. In a first attempt, we investigated the potency of the general antioxidant and ROS-scavenger N-acetylcysteine (NAC) [32–34]. NAC potently diminished the oxidation of Amplex Red by HOBr already at low (micromolar) concentrations
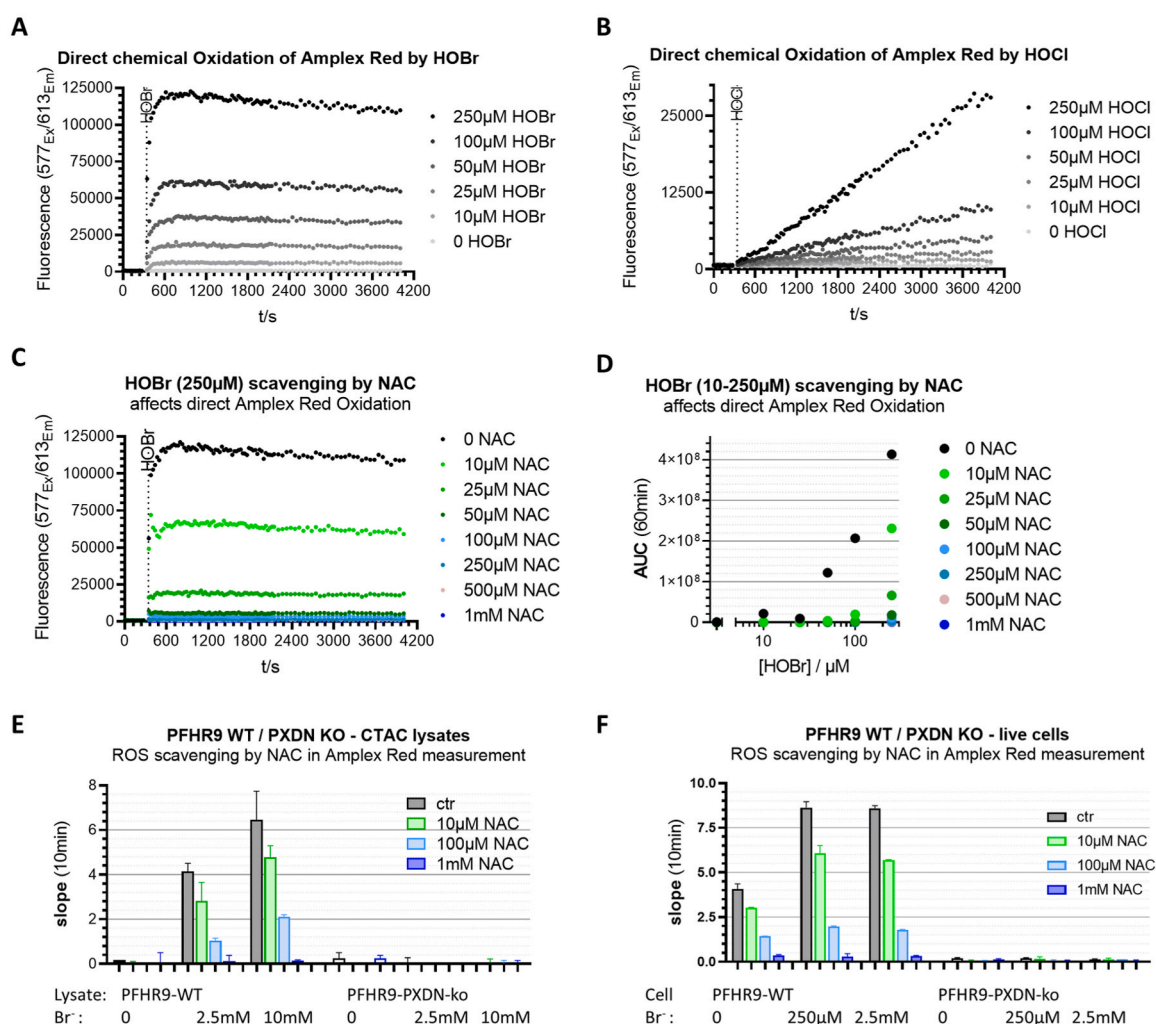

Fig. 4. Direct oxidation of Amplex Red dye to resorufin by HOBr (A) and HOCl (B). N-acetylcystein (NAC, C,D) diminishes oxidation of Amplex Red by HOBr in a dose dependent manner. Exemplarily, the impact on the oxidation of 50 μM Amplex Red by 250 μM HOBr is shown in the presence of increasing NAC (C) concentrations. Areas under the curves following a 1 h reaction time with Amplex Red are shown for the interaction of further concentrations of HOBr with NAC (D). In Amplex Red assays performed with CTAC lysates (E), as well as with intact (F) PFHR-9 WT (filled columns), but not for PXDN-KO (open columns) cells, the bromide enhanced signal was attenuated. Carnosine scavenges hypohalous acids, by halogenation reactions. (For interpretation of the references to color in this figure legend, the reader is referred to the Web version of this article.)

(Fig. 4C and D). In line with this, also in CTAC lysates of PFHR-9-WT cells, supplemented with bromide, a dose dependent decrease in fluorescence could be observed, while NAC supplementation did not affect the signal obtained from CTAC lysates of PFHR-9-PXDN-KO cells (Fig. 4E). Comparable results were obtained for Amplex Red assays performed on intact PFHR-9-WT and PXDN-KO cells (Fig. 4F). However, it should be noted, that for experiments performed on intact cells, NAC supplementation also largely diminished the signal obtained in the absence of additional bromide (Fig. 4F). This may be explained by the fact that NAC is a rather strong and not too selective antioxidant, that presumably also scavenges added H_2O_2.

Carnosine, by contrast is a dipeptide, found in high concentrations in muscle (up to 20 mM in human) and in the brain (up to 5 mM) under physiological conditions [35]. Carnosine has been suggested to scavenge HOCl and HOBr by directly being halogenated to chloramines or bromamines, respectively [36,37]. Therefore, it might serve as a more selective scavenging reagent. Indeed, carnosine interferes with oxidation of Amplex Red by HOBr (Fig. 5A and B), and HOCl (Figure S5). Given the very fast nature of Amplex Red oxidation by HOBr, a full scavenging could not be achieved, when HOBr was added to a mixture of carnosine and Amplex Red (Fig. 5A and B). In contrast to that direct interaction (filled symbols, Fig. 5C), when carnosine was allowed to
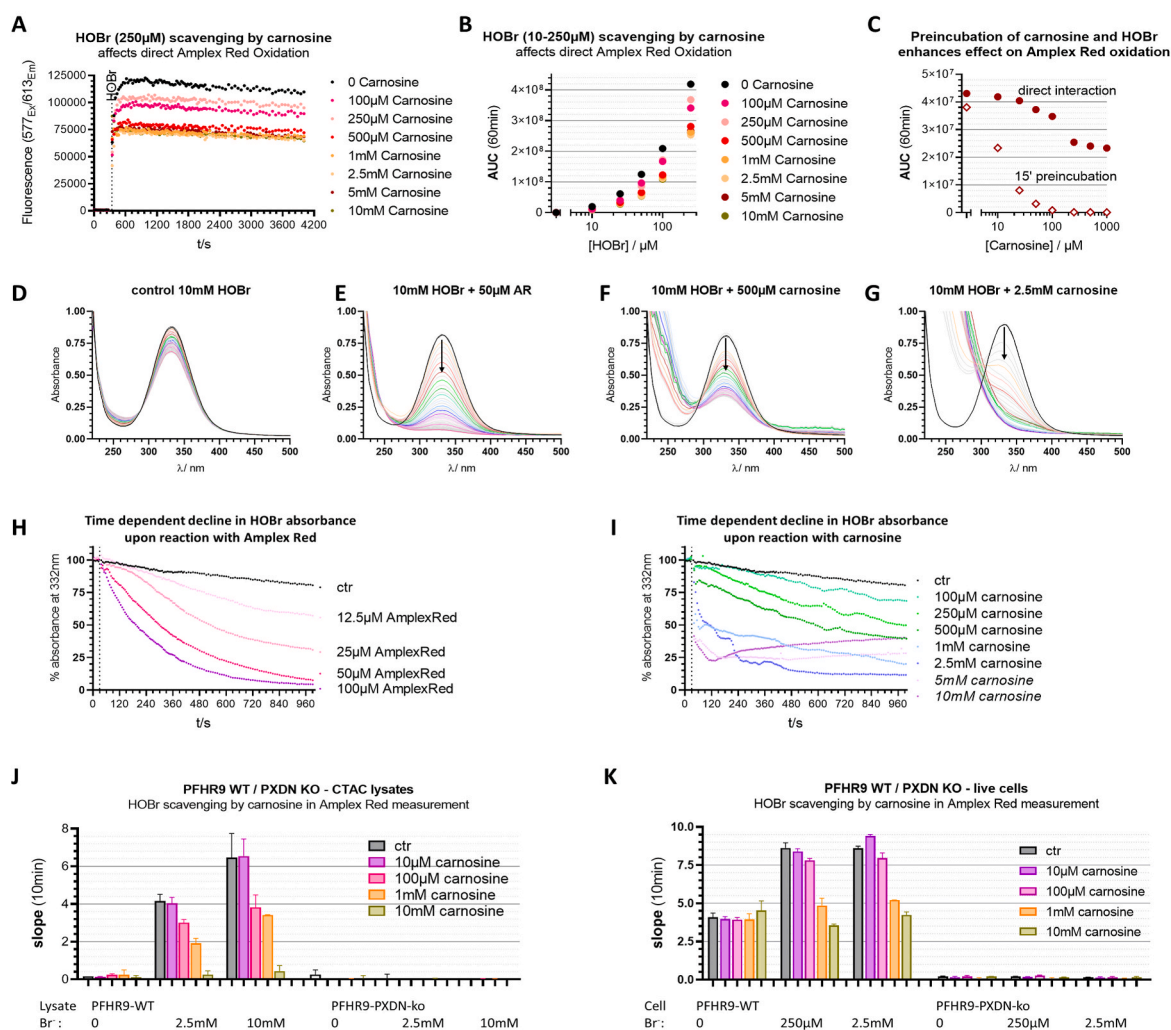

Fig. 5. The direct effect of increasing carnosine concentrations on the oxidation of 50 μM Amplex Red by 250 μM HOBr is shown exemplarily (A), and areas under the curves following a 1 h reaction time are shown for the interaction of further concentrations of HOBr with carnosine (B). Areas under curves decrease with increasing carnosine concentrations to 50% of initial fluorescence when HOBr is added to a mixture of Amplex Red and carnosine (filled symbols, panel C), but go down completely, when carnosine is allowed to react for 15 min prior to addition of Amplex Red (open symbols, panel C) at a twofold excess of carnosine over Amplex Red. The reactivity of Amplex Red and carnosine towards oxidation by HOBr is illustrated by changes in the absorbance spectra of 10 mM HOBr, reacted with indicated concentrations of Amplex Red (E,H) or carnosine (F,G,I). Absorbance spectra were recorded every 5 s in the range from 220 nm to 500 nm over a time frame of 15–20 min. Panels D–G exemplarily show spectra of the reaction with 50 μM Amplex Red (E), 500 μM (F) and 2.5 mM carnosine (G) in comparison to HOBr decline without added reagents (D). Spectra are highlighted to illustrate changes upon addition of the scavenger for the indicated times in orange: 0.5min, light red: 1.5min, bright red: 2.5min, dark red: 3.5min, light green: 4.5min, dark green: 5.5min, cyan: 6.5min, very light blue: 7.5 min, light blue: 8.5min, blue: 9.5min, dark purple: 10.5min, light purple: 11.5min, light rose: 12.5min, rose: 14.5min, pink: 19.5min. Spectra showing the interaction of HOBr with further concentrations of Amplex Red are shown in Figure S6, those showing the interaction with further concentrations of carnosine are shown in Figure S7. Decline in absorbance at 332 nm implies the reaction of HOBr upon addition of Amplex Red (H) or carnosine (I), indicated by the dotted line. Of note, at high concentrations of carnosine (5 mM and 10 mM), an increase in absorbance at 332 nm can be observed, which is due to the formation of the carnosine derived bromamine. In Amplex Red assays performed with CTAC lysates (J), as well as with intact (K) PFHR-9 WT (filled columns), but not for PXDN-KO (open columns) cells, the bromide enhanced signal was attenuated by co-administration of carnosine. Displayed results show a representative experiment out of three independent experiments performed in duplicates. (For interpretation of the references to color in this figure legend, the reader is referred to the Web version of this article.)

react with HOBr shortly prior to addition of Amplex Red, a full scavenging could be observed at a twofold excess of carnosine over Amplex Red (open symbols, Fig. 5C). This might suggest that the reaction with carnosine is slower compared to the oxidation of Amplex Red, and that the carnosine derived bromamine does not react with Amplex Red. In order to follow up on this observation, we monitored the decline in HOBr absorbance upon mixture with increasing concentrations of Amplex Red (Fig. 5E,H) or carnosine (Fig. 5F,G,I), respectively. It should be noted, that the concentration of HOBr necessary to detect changes in the absorbance spectra is much higher than the concentration used in previous measurements and by far exceeds the physiological relevant concentrations. However, compared to that high HOBr concentration, relatively small amounts of Amplex Red and carnosine are able to scavenge HOBr. While in a reaction with 50 μM Amplex Red, as usually used for assay, the 10 mM of HOBr are completely used up to oxidize the dye within 15–20 min (Fig. 5E,H), reaction with a tenfold higher concentration of carnosine proceeds much slower (Fig. 5F,I). To compare the reactivity, the absorbance maximum of the HOBr spectrum (at 332 nm) is shown as a function of time for the reaction with increasing concentrations of Amplex Red (Fig. 5H) and carnosine (Fig. 5I), respectively.

In CTAC lysates of PFHR-9-WT cells supplemented with bromide, a dose dependent scavenging effect of carnosine could be observed, while co-administration of carnosine did not affect signals obtained from CTAC lysates of PFHR-9-PXDN-KO cells (Fig. 5J). Even though observed at higher concentrations, the measure of the effect is comparable to that observed with NAC (Fig. 4E). Likewise, a dose dependent scavenging effect of carnosine could also be observed when it was co-administered

to intact cells PFHR-9-WT, but not to PFHR-9-PXDN-KO cells (Fig. 5K). In contrast to the effect of NAC (Fig. 4F), for intact cells (Fig. 5K), carnosine did not affect Amplex Red oxidation in the absence of bromide. In the presence of bromide, however, a dose dependent scavenging could be observed, that decreased the fluorescence to the level obtained without bromide supplementation, suggesting that indeed HOBr might be responsible for the bromide enhancing effect of Amplex Red fluorescence.

Comparable scavenging effects could be observed for CTAC lysates and intact cells of the PXDN-rescue cell line PFHR-9-Resc-wt, but not for the non-functional PXDN mutant expressing cell line PFHR-9-Resc-mut (Figure S8).

The here presented differences in the kinetics of the reaction of Amplex Red and carnosine with HOBr might suggest that the initial drop observed in PXDN activity in bromide free H-medium upon addition of increasing concentrations of bromide (Fig. 2H) could be due to a competition between Amplex Red and bromide as substrates for PXDN. A detailed description is offered in the supporting information (Figure S9).

Of note, while similar to PXDN, also LPO is able to oxidize bromide to HOBr, a bromide mediated signal enhancement was not observed when the Amplex Red assay was performed on purified LPO (Figure S10).

3.6. Measurement of PXDN activity in human coronary and aortic smooth muscle cells (HCSMCs and HAoSMCs)

While PFHR-9 cells produce large amounts of ECM, also primary cells express PXDN and we wanted to explore whether measurement of PXDN
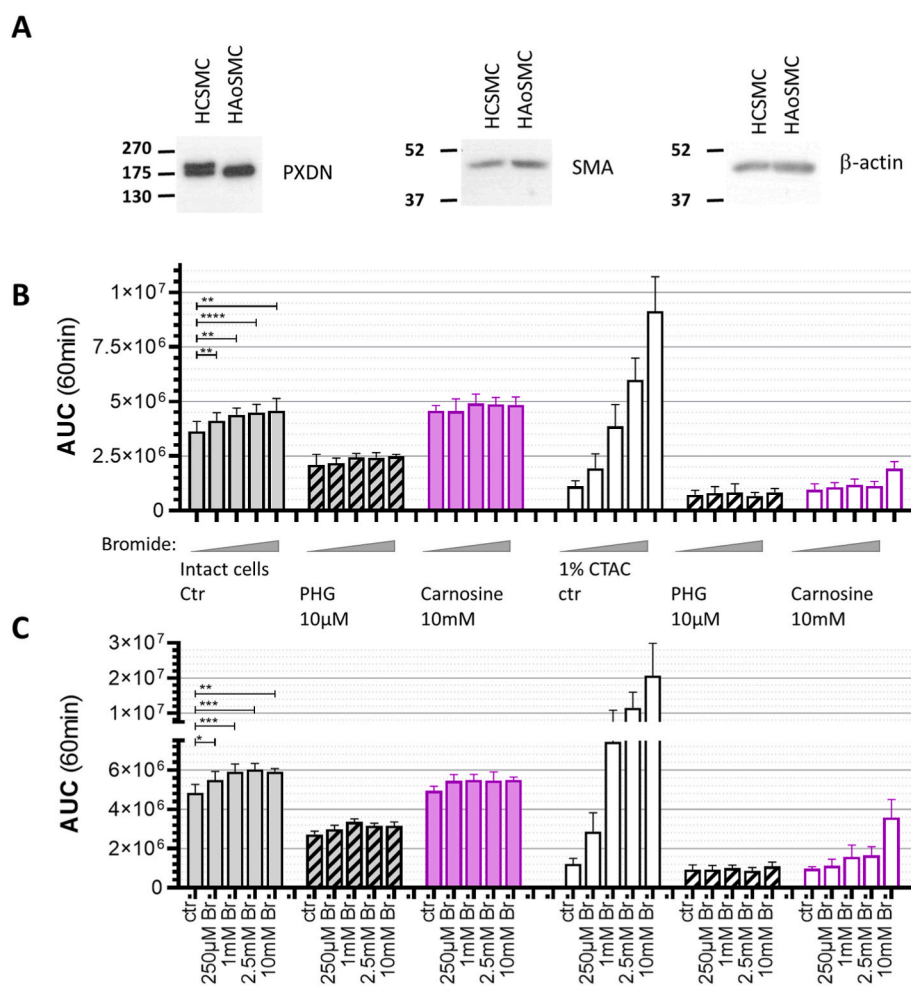

Fig. 6. Peroxidasin expression in HCSMCs and HAoSMCs is shown by western blots next to smooth muscle actin (SMA) and β-actin (A). Amplex Red assay measured on HCSMCs (B) and HAoSMCs (C) in bromide-free H-medium with increasing concentrations of bromide (0, 250 μM, 1 mM, 2.5 mM, 10 mM). Areas under the curves are calculated and shown for intact cells (filled columns) and for cells lysed with 1% CTAC (open columns) in control conditions (grey), as well as in the presence of 10 μM PHG (hatched), or 10 mM carnosine (purple). Data represent mean with SD of three (B), or two (C) independent experiments performed in duplicates. Significance was calculated by *t*-test; results are given as *: p ≤ 0.05, **: p ≤ 0.01, ***: p ≤ 0.001, ****: p ≤ 0.0001. (For interpretation of the references to color in this figure legend, the reader is referred to the Web version of this article.)

activity is feasible for human vascular smooth muscle cells.

Western blots confirm the expression of PXDN in human coronary smooth muscle cells (HCSMCs) and human aortic smooth muscle cells (HAoSMCs, Fig. 6A), while the expression of smooth muscle actin indicates the SMC phenotype (Fig. 6A). Having confirmed the presence of

PXDN in these cells, we aimed to measure its activity in intact cells as well as in cell lysates (1% CTAC) and the effect of bromide amplification. With both, HCSMCs (Fig. 6B) and HAoSMCs (Fig. 6C), a slight dose dependent increase in Amplex Red fluorescence is observed by addition of bromide to intact cells. As observed for PFHR-9 cells, cell lysis with
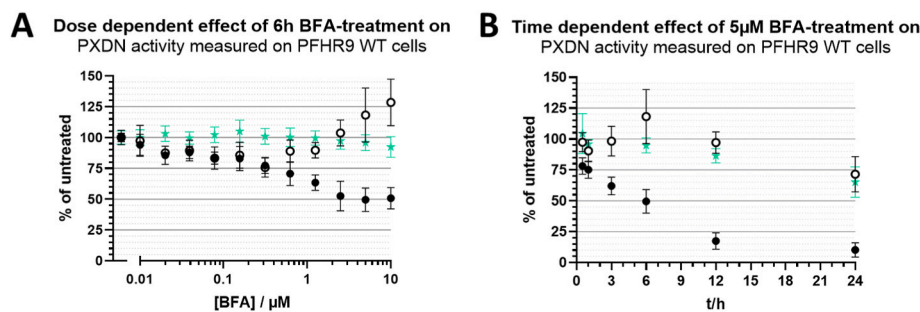

Fig. 7. Brefeldin A inhibits secretion of PXDN. Area under curves of a 1 h time course from Amplex Red oxidation (50 μM, in the presence of 2.5 mM bromide and 50 μM H$_2$O$_2$), obtained from intact (filled circles), and CTAC lysed (open circles) PFHR-9-WT cells treated with increasing concentrations of BFA were normalized to untreated controls for 6 h (A). Time dependence of the effect is shown exemplarily for incubation with 5 μM BFA (B). After experiments, total protein amount was measured by Bradford assay to exclude artifacts due to uneven cell growth or toxicity of the treatments (cyan stars, panels A, B). Results show mean and standard deviation of 2–4 independent experiments, performed in duplicates. Immunostaining using our monoclonal anti-PXDN antibody shows inhibited secretion of PXDN in PFHR-9 WT cells treated with 5 μM BFA for 12 h (C). Activity of PXDN could be monitored in decellularized ECM of PFHR-9 WT (but not of PXDN-KO) cells (50 μM Amplex Red, 50 μM H$_2$O$_2$), with signal amplification with increasing bromide concentrations (absence of bromide: grey, 250 μM: orange, 2.5 mM: red, 25 mM: bordeaux). Treatment with 5 μM BFA decreased measurable PXDN activity m the decellularized ECM. Presented data show results of a representative experiment out of four. (For interpretation of the references to color in this figure legend, the reader is referred to the Web version of this article.)
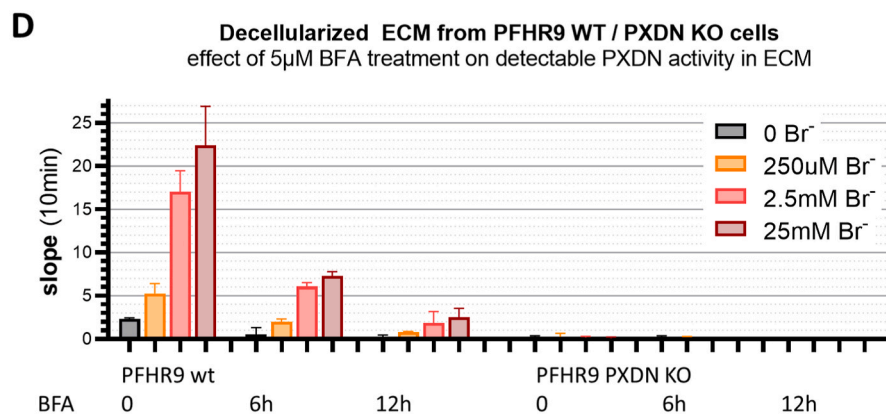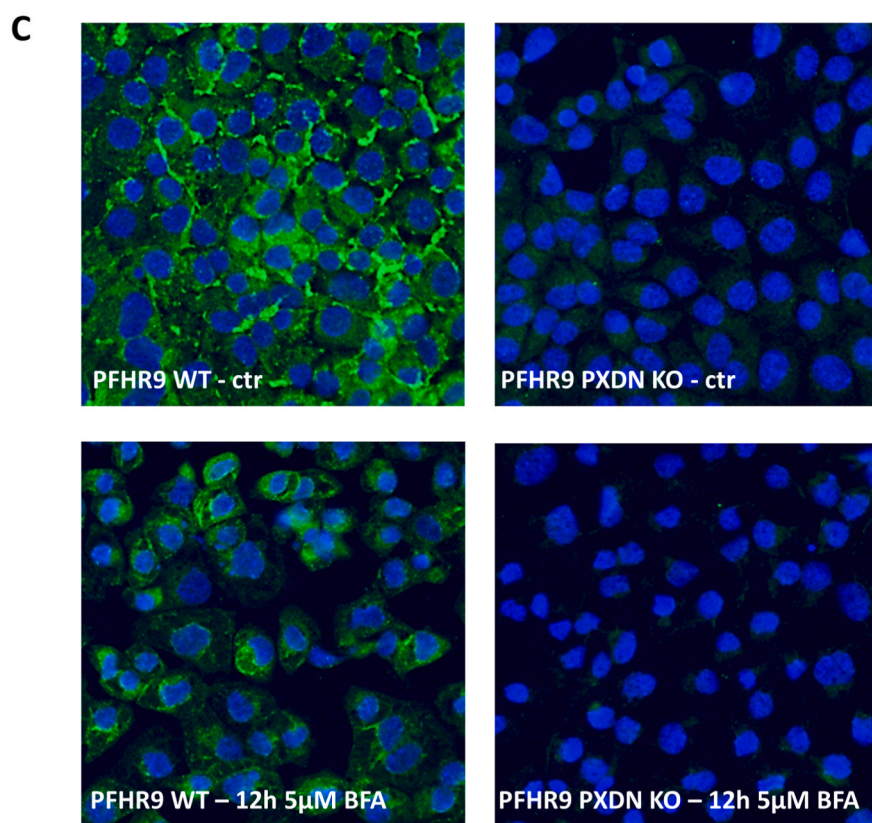
1% CTAC decreased Amplex Red oxidation in the absence of bromide and enhanced the bromide amplification of the signal. An additional factor contributing to the higher signal in smooth muscle lysates may be the localization of PXDN to intracellular compartments, which was previously demonstrated in human dermal and pulmonary myofibroblasts [17]. The intracellular PXDN pools, co-localizing with the ER and Golgi, are probably not accessible to the assay in intact cells.

The signal enhancing effect of bromide in both intact cells and CTAC lysates, is abrogated in the presence of the PXDN-inhibitor PHG (hatched columns in Fig. 6B,C) and in the presence of the HOBr scavenger carnosine (purple columns in Fig. 6B,C).

3.7. Monitoring of altered PXDN secretion using the modified Amplex Red assay

Interestingly, while for SMCs, lysis with CTAC largely increased the fluorescence observed in the presence of bromide, for PFHR-9 cells, the opposite seems to be the case as here fluorescence in intact cells was higher than in lysates (*vide supra*).

This intriguing difference might be due to differences in secretion, since the Amplex Red assay will detect extracellular peroxidase activity. Hence, we wanted to see whether the modification of the Amplex Red assay using bromide for signal amplification enabled us to study effects of PXDN trafficking on intact cells. To that aim, we incubated cells with Brefeldin A (BFA), a well-known inhibitor of ER-Golgi transport [38,39].

Indeed, with increasing BFA concentrations (Fig. 7A) we observed decreased Amplex Red oxidation in intact cells (filled circles). Exemplarily, in Fig. 7A, the dose dependent effect upon a 6 h treatment is shown. Dose dependent results for further incubation times are shown in the supplement (Figure S11). In order to exclude that PXDN expression was compromised upon treatment, we lysed half of the samples with CTAC for the Amplex Red assay. Strikingly, in the presence of CTAC, no major decrease in Amplex Red oxidation was observed upon BFA treatment. In contrast, a slight increase could be observed at higher concentrations, depending on the incubation time (Fig. 7A, S11). The increase may be related to the intracellular accumulation of PXDN due to inhibited secretion. Time dependence of the effect is shown exemplarily for incubation with 5 µM BFA (Fig. 7B), as well as for 1.25 and 2.5 µM (Figure S12). Similar effects were observed, when cells were seeded in higher confluence, though higher concentrations were necessary, to obtain comparable results (Figure S12).

In order to confirm the effect of BFA on PXDN retaining in the ER, we imaged PXDN using the anti-PXDN monoclonal antibody (Fig. 7C). It is apparent, that PXDN signal is higher in untreated PFHR-9 WT cells (upper left panel) as compared to cells treated for 12 h with 5 µM BFA (lower left panel). Furthermore, in the treated cells, the fluorescence pattern shows a more reticular structure, while in the untreated control a more homogenous cellular and extracellular distribution is apparent.

To further confirm the effect of BFA, we decellularized the ECM of PFHR-9 WT and PXDN-KO cells treated with BFA and monitored PXDN activity in the matrix with Amplex Red assay in the presence of increasing concentrations of bromide (Fig. 7D). In line with the previous observations, less PXDN activity is detectable from decellularized ECM upon treatment with BFA in a time dependent manner.

4. Discussion

Basement membranes are essential for normal development and function of diverse tissues and cells. Alterations in basement membrane function are frequently observed in the pathogenesis of several diseases including Goodpasture's and Alport syndrome [7], as well as in cancer [8,40–42] and organ fibrosis [9,17]. PXDN has recently emerged as a key component of basement membranes providing a link between oxidant production and ECM modification in animals.

Diverse methods have been reported to study the activity of PXDN. Since PXDN mediates the crosslinking of collagen IV, an isolation and purification of collagen IV NC1 hexamers after collagenase digestion enables the investigation of PXDN activity by revealing cross-linked dimeric and uncrosslinked monomeric subunits of collagen IV in Coomassie-stained SDS gels [11]. The purification step could be omitted if digests of hypotonic cell lysates are directly applied to western blotting for the subsequent detection of monomeric and dimeric collagen IV subunits [13,18,21]. PXDN derived HOBr can brominate organic substances, thus formation of NADH-bromohydrin and 3-bromotyrosine could be used to detect PXDN activity in decellularized ECM by Liquid Chromatography-tandem mass spectrometry (LC/MS/MS) [15,20].

However, these methods require either laborious sample preparation or special equipment and are not suited to study a large number of samples or a direct effect on PXDN activity in cellular physiological environment. Peroxidase assays have been used to study the activity of purified PXDN, following e.g. the oxidation of o-dianisidine and tyrosine [4], or tetramethylbenzidine [19]. Also, the Amplex Red assay has been applied to measure PXDN activity in CTAB lysates [17,18], as well as in isolated decellularized ECM [20].

Here, we describe a modification of the Amplex Red assay that enables the measurement of PXDN activity in live cells, providing a useful tool to study PXDN activity in a physiological context. We provide insight into the mechanism of signal amplification and demonstrate that alterations in PXDN secretion can be measured in live cells using our method.

When we measured the peroxidase activity of cell lysates, we observed that a change of counter-anion of the detergent CTAB from bromide to chloride (to CTAC) completely abrogated Amplex Red oxidation in cell lysates of PFHR-9-WT cells. However, supplementing CTAC lysates with bromide could restore fluorescence in a dose dependent manner. In line with this, in a recent article, Pauman-Page et al. have noted that addition of bromide to lysates they applied in their functional assays increased the obtained signal [40]. We could also measure PXDN activity on intact PFHR-9-WT cells, especially when they were allowed to reach an over-confluent state. Addition of bromide to the assay buffer strongly amplified the signal obtained from intact PFHR-9 WT cells in a dose dependent manner. Since Amplex Red is a substrate for multiple heme peroxidases, we applied several genetic tools to confirm the involvement of PXDN in the observed amplification of Amplex Red oxidation by bromide. We did not detect any Amplex Red oxidation in PFHR-9 cells, where the PXDN gene was disrupted by the CRISPR/Cas9 technique. In order to exclude the possibility that this might be related to the clonal selection process, we confirmed the importance of PXDN, by using a specific PXDN targeting siRNA. Furthermore, re-introduction of PXDN to PXDN deficient PFHR-9 cells was able to partially restore the signal (Resc-wt cells), in coherence with a lower expression as compared to the PFHR-9 WT cells. We previously showed that Q823W and D826E mutations, which disturb halide binding and the covalent link formation to the heme center, respectively [43], abrogated the peroxidase activity of PXDN [13,18]. Hence, introducing a non-functional mutant did not restore Amplex Red oxidation (Resc-mut cells). Taken together, these data suggest, that PXDN is indeed responsible for the observed signal amplification of Amplex Red oxidation by bromide.

Bromide is essential for the cross-linking of collagen IV [10]. Upon oxidation of its heme center by H_2O_2 (to the oxo-ferryl form 'compound 1'), PXDN catalyzes the oxidation of bromide to hypobromous acid (HOBr) [1]. HOBr in turn oxidizes methionine 93 of collagen IV, to form a bromo-sulfonium cation that is then nucleophilically attacked by the nitrogen of (hydroxyl)lysine 211, forming a sulfilimine bond. Currently, this is the only known example for sulfilimine bond formation in living organisms [9].

When this mechanism was first described, also the formation of a chlorosulfonium cation was envisaged, suggesting a potential role of HOCl in the catalysis. However, a catalysis by HOCl seems not to be feasible, as the chloro-sulfonium cation of methionine would rather be prone to a nucleophilic attack by water than by the lysine nitrogen,

resulting in sulfoxide rather than a cross-linked sulfilimine [6,10]. While in comparison to the trace element bromide, chloride is much more abundant in plasma (50–100 μM Br$^-$ vs 95–105 mM Cl$^-$, respectively [6]), PXDN has a high substrate specificity, preventing collateral damage through excess HOCl production. Kinetic studies showed that PXDN cannot oxidize chloride: while thiocyanate, iodide and bromide, acting as two-electron donors, efficiently restored the ferric state of the enzyme, chloride was not able to act as a two-electron donor of compound 1 [14]. In line with this, we do not observe PXDN activity in CTAC lysates without bromide supplementation.

Trace amounts of bromide present in commercial salts have been shown to be sufficient to mediate cross-linking of collagen IV [10]. Hence, we applied a bromide free buffer, replacing the commercial sodium and potassium chlorides with synthesized ones following a the protocol of McCall et al. [10]. Despite the significant signal amplification by bromide in the Amplex Red assays performed on intact PFHR-9 WT (and PFHR-9-Resc-wt) cells, also in the absence of bromide (a PHG-sensitive) oxidation of Amplex Red could be observed.

We hypothesized that in the absence of bromide, Amplex Red as a one electron donor [31], is oxidized by PXDN in the peroxidase cycle of the enzyme [1,30], while in contrast, in the presence of bromide, preferably HOBr would be formed, which might then oxidize Amplex Red directly, resulting in a signal amplification. We show that HOBr indeed reacts with Amplex Red very quickly and that scavengers like N-acetylcysteine and carnosine diminish Amplex Red oxidation by HOBr. Carnosine is halogenated by hypohalous acids and thus serves as a more specific scavenger as compared to the general N-acetylcysteine. While Amplex Red is oxidized by HOBr very efficiently and very quickly, the reaction with carnosine is considerably slower, thus the direct HOBr scavenging effect of carnosine on Amplex Red oxidation is less efficient than in a condition where HOBr is allowed to react with carnosine prior to addition of Amplex Red (as the carnosine derived bromamine does not seem to oxidize Amplex Red). Of note, the concentrations used to study the chemical interaction of HOBr, the respective scavengers and Amplex Red exceed those present in the physiological milieu by far. In line with this both scavengers efficiently diminished Amplex Red oxidation by PXDN in cell lysates and in intact cells.

The enzymatic redox intermediate compound 1 links both, the halogenation and the peroxidase cycle of PXDN and it has been shown for several endogenous one-electron donors, that concentration of the respective substrates as well as their rate constants for the reduction of compound 1 dictate under which cycle the enzyme will operate [44]. Addition of smaller concentrations of bromide to bromide free buffer slightly decreased the formation of the fluorescent Amplex Red oxidation product resorufin, which might indicate a competition, and a possible shift from Amplex Red oxidation to bromide oxidation. While HOBr quickly oxidizes Amplex Red, the reducing environment of the cell might scavenge and disarm low amounts of HOBr, suggesting that in a cellular context, a certain amount of HOBr must be produced before an enhancing effect becomes apparent. An increase of this effect in lower cell density and a decrease in higher concentrations of Amplex Red support this theory further.

Importantly, a bromide mediated signal enhancement could not be obtained in Amplex Red assays performed with purified LPO, suggesting that this method might indeed be specific for measurements of PXDN activity. This is in line with a reported substrate selectivity: while next to PXDN, also LPO is able to oxidize bromide to HOBr, based on second order rate constants of compound 1 formation, PXDN outperforms the reactivity of LPO towards bromide by more than two orders of magnitude (560×10^4 M^{-1}s^{-1} for PXDN *vs.* 4.1×10^4 M^{-1}s^{-1} for LPO, respectively) [14]. These results suggest that bromide amplification of Amplex Red assay might be specifically used for the measurement of PXDN activity in mammalian cells. We did not investigate the effect of bromide on measurable activity of EPO, which based on its apparent second-order rate constant (1900×10^4 M^{-1}s^{-1}) should also show signal amplification in the presence of bromide in the Amplex Red assay [14].

However, the expression of EPO is highly restricted to eosinophil granulocytes and in line with this, of the 69 cell lines listed in the Human Protein Atlas (www.proteinatlas.org), the acute promyelocytic leukemia cell line NB-4 was the only one showing EPO expression on mRNA level.

Interestingly, in PFHR-9 cells, the obtained resorufin signals were overall higher in intact cells as compared to cell lysates. Similarly, a recent study suggests, that a higher concentration of bromide was needed to observe comparable levels of collagen IV crosslinking from isolated PFHR-9 ECM when compared to cultured cells, possibly suggesting a bromide accumulation at the site of collagen IV crosslinking in live cells, which results in a higher effective concentration than that of the medium, while this compartmentalization is lost during isolation of ECM [15].

PXDN localizes to the ER and is secreted into the extracellular space in a regulated manner [17]. In stark contrast to the PFHR-9 cells, which are producing large amounts of ECM and constantly secreting PXDN, in human coronary and human aortic smooth muscle cells, a higher amplification of Amplex Red oxidation was observed in CTAC lysates as compared to intact cells. While the extend of amplification on intact smooth muscle cells was lower as compared to their lysates, also here a bromide mediated amplification of Amplex Red oxidation by PXDN could be confirmed. This effect could be annihilated by inhibition of PXDN with PHG or by scavenging of HOBr with carnosine. Taken together, these data suggests that the majority of PXDN pools in smooth muscle cells is intracellular, and thus not accessible for the extracellular reaction with Amplex Red.

Other dyes like aminophenyl fluorescein (APF, 2-[6-(4′-amino)phenoxy-3H-xanthen-3-on-9-yl)benzoic acid) and hydroxyphenyl fluorescein (HPF, 2-[6-(4′-hydroxy)phenoxy-3H-xanthen-3-on-9yl)benzoic acid) have been applied to detect hypohalous acids in biological setups and might offer the advantage of being cell permeable [45,46]. However, since PXDN is largely secreted to the extracellular space, and its main function of collagen IV crosslinking is likely to take place in the extracellular space, being able to specifically measure extracellular PXDN activity can be seen as an advantage. Furthermore, comparing measured PXDN activity in intact *vs.* lysed cells can provide information about the distribution of the enzyme between the intra- and extracellular space. In order to investigate this question further and to validate the modified assay, we applied BFA, a well-known inhibitor of ER-Golgi transport. Indeed, measurement of PXDN activity in living cells allowed us to track changes in PXDN secretion. To demonstrate that, we showed that BFA effectively inhibited the release of PXDN from PFHR-9 WT cells, which was confirmed by PXDN immunostaining and measuring PXDN activity of decellularized ECM. Although BFA is a pharmacological tool which we used to study the trafficking of PXDN, the here described method enables the investigation of hitherto unknown physiological modulators of PXDN synthesis and secretion. Thus, the described measuring tool opens up new opportunities to study PXDN activity in physiological context, and to investigate the effect of receptor agonists and inhibitors, as well as pharmacological compounds on PXDN secretion and activity. These future experiments might provide a better understanding of the processes mediating the extracellular modification of collagen IV.

5. Conclusion

Here, we report for the first time the measurement of PXDN activity on intact cells. Addition of bromide leads to signal amplification in the Amplex Red assay, most likely due to PXDN mediated production of HOBr, that quickly oxidizes Amplex Red to resorufin. Inhibition of PXDN, as well as scavenging of HOBr by carnosine abrogates this amplification. In smooth muscle cells, in which the larger fraction of PXDN is intracellular, the bromide enhancement is more pronounced in lysates as compared to intact cells.

Applying bromide amplification, the Amplex Red assay can serve as a versatile tool to study PXDN activity in live cells, and investigate

biological questions and processes related to e.g. protein trafficking.

Funding

Declaration of competing interest

The authors declare no conflict of interest.

Appendix A. Supplementary data

Supplementary data to this article can be found online at https://doi.org/10.1016/j.redox.2022.102385.

References

[1] M.J. Davies, C.L. Hawkins, D.I. Pattison, M.D. Rees, Mammalian heme peroxidases: from molecular mechanisms to health implications, Antioxidants Redox Signal. 10 (2008) 1199–1234, https://doi.org/10.1089/ars.2007.1927.

[2] M. Zamocky, C. Jakopitsch, P.G. Furtmüller, C. Dunand, C. Obinger, The peroxidase–cyclooxygenase superfamily: reconstructed evolution of critical enzymes of the innate immune system, Proteins: Struct., Funct., Bioinf. 72 (2008) 589–605, https://doi.org/10.1002/prot.21950.

[3] C.A. Foerder, B.M. Shapiro, Release of ovoperoxidase from sea urchin eggs hardens the fertilization membrane with tyrosine crosslinks, Proc. Natl. Acad. Sci. USA 74 (1977) 4214–4218, https://doi.org/10.1073/pnas.74.10.4214.

[4] R.e. Nelson, L.i. Fessler, Y. Takagi, B. Blumberg, D.r. Keene, P.f. Olson, C.g. Parker, J.h. Fessler, Peroxidasin: a novel enzyme-matrix protein of Drosophila development, EMBO J. 13 (1994) 3438–3447, https://doi.org/10.1002/j.1460-2075.1994.tb06649.x.

[5] G. Sirokmány, H.A. Kovács, M. Geiszt, Peroxidasin: structure and function, in: Mammalian Heme Peroxidases, CRC Press, 2021.

[6] S. Colon, P. Page-McCaw, G. Bhave, Role of hypohalous acids in basement membrane homeostasis, Antioxidants Redox Signal. 27 (2017) 839–854, https://doi.org/10.1089/ars.2017.7245.

[7] A. Pozzi, P.D. Yurchenco, R.V. Iozzo, The nature and biology of basement membranes, Matrix Biol. (2017) 1–11, https://doi.org/10.1016/j.matbio.2016.12.009, 57–58.

[8] Z. Péterfi, M. Geiszt, Peroxidasins: novel players in tissue genesis, Trends Biochem. Sci. 39 (2014) 305–307, https://doi.org/10.1016/j.tibs.2014.05.005.

[9] M. Pehrsson, J.H. Mortensen, T. Manon-Jensen, A.-C. Bay-Jensen, M.A. Karsdal, M. J. Davies, Enzymatic cross-linking of collagens in organ fibrosis – resolution and assessment, Expert Rev. Mol. Diagn. 21 (2021) 1049–1064, https://doi.org/10.1080/14737159.2021.1962711.

[10] A.S. McCall, C.F. Cummings, G. Bhave, R. Vanacore, A. Page-McCaw, B.G. Hudson, Bromine is an essential trace element for assembly of collagen IV scaffolds in tissue development and architecture, Cell 157 (2014) 1380–1392, https://doi.org/10.1016/j.cell.2014.05.009.

[11] G. Bhave, C.F. Cummings, R.M. Vanacore, C. Kumagai-Cresse, I.A. Ero-Tolliver, M. Rafi, J.-S. Kang, V. Pedchenko, L.I. Fessler, J.H. Fessler, B.G. Hudson, Peroxidasin forms sulfilimine chemical bonds using hypohalous acids in tissue genesis, Nat. Chem. Biol. 8 (2012) 784–790, https://doi.org/10.1038/nchembio.1038.

[12] G. Bhave, S. Colon, N. Ferrell, The sulfilimine cross-link of collagen IV contributes to kidney tubular basement membrane stiffness, Am. J. Physiol. Ren. Physiol. 313 (2017) F596–F602, https://doi.org/10.1152/ajprenal.00096.2017.

[13] H.A. Kovács, E. Lázár, G. Várady, G. Sirokmány, M. Geiszt, Characterization of the proprotein convertase-mediated processing of peroxidasin and peroxidasin-like protein, Antioxidants 10 (2021) 1565, https://doi.org/10.3390/antiox10101565.

[14] M. Paumann-Page, R.-S. Katz, M. Bellei, I. Schwartz, E. Edenhofer, B. Sevcnik, M. Soudi, S. Hofbauer, G. Battistuzzi, P.G. Furtmüller, C. Obinger, Pre-steady-state kinetics reveal the substrate specificity and mechanism of halide oxidation of truncated human peroxidasin 1, J. Biol. Chem. 292 (2017) 4583–4592, https://doi.org/10.1074/jbc.M117.775213.

[15] B. Bathish, M. Paumann-Page, L.N. Paton, A.J. Kettle, C.C. Winterbourn, Peroxidasin mediates bromination of tyrosine residues in the extracellular matrix, J. Biol. Chem. (2020), https://doi.org/10.1074/jbc.RA120.014504 jbc. RA120.014504.

[16] C. He, W. Song, T.A. Weston, C. Tran, I. Kurtz, J.E. Zuckerman, P. Guagliardo, J. H. Miner, S.V. Ivanov, J. Bougoure, B.G. Hudson, S. Colon, P.A. Voziyan, G. Bhave, L.G. Fong, S.G. Young, H. Jiang, Peroxidasin-mediated bromine enrichment of

[17] Z. Péterfi, Á. Donkó, A. Orient, A. Sum, Á. Prókai, B. Molnár, Z. Veréb, É. Rajnavölgyi, K.J. Kovács, V. Müller, A.J. Szabó, M. Geiszt, Peroxidasin is secreted and incorporated into the extracellular matrix of myofibroblasts and fibrotic kidney, Am. J. Pathol. 175 (2009) 725–735, https://doi.org/10.2353/ajpath.2009.080693.

[18] E. Lázár, Z. Péterfi, G. Sirokmány, H.A. Kovács, E. Klement, K.F. Medzihradszky, M. Geiszt, Structure–function analysis of peroxidasin provides insight into the mechanism of collagen IV crosslinking, Free Radic. Biol. Med. 83 (2015) 273–282, https://doi.org/10.1016/j.freeradbiomed.2015.02.015.

[19] S. Colon, G. Bhave, Proprotein convertase processing enhances peroxidasin activity to reinforce collagen IV, J. Biol. Chem. 291 (2016) 24009–24016, https://doi.org/10.1074/jbc.M116.745935.

[20] B. Bathish, R. Turner, M. Paumann-Page, A.J. Kettle, C.C. Winterbourn, Characterisation of peroxidasin activity in isolated extracellular matrix and direct detection of hypobromous acid formation, Arch. Biochem. Biophys. 646 (2018) 120–127, https://doi.org/10.1016/j.abb.2018.03.038.

[21] G. Sirokmány, H.A. Kovács, E. Lázár, K. Kónya, Á. Donkó, B. Enyedi, H. Grasberger, M. Geiszt, Peroxidasin-mediated crosslinking of collagen IV is independent of NADPH oxidases, Redox Biol. 16 (2018) 314–321, https://doi.org/10.1016/j.redox.2018.03.009.

[22] Z. Izsvák, M.K.L. Chuah, T. VandenDriessche, Z. Ivics, Efficient stable gene transfer into human cells by the Sleeping Beauty transposon vectors, Methods 49 (2009) 287–297, https://doi.org/10.1016/j.ymeth.2009.07.001.

[23] Z. Schneider, J. Cervenak, M. Baranyi, K. Papp, J. Prechl, G. László, A. Erdei, I. Kacskovics, Transgenic expression of bovine neonatal Fc receptor in mice boosts immune response and improves hybridoma production efficiency without any sign of autoimmunity, Immunol. Lett. 137 (2011) 62–69, https://doi.org/10.1016/j.imlet.2011.02.018.

[24] Inc. GraphPad Software, GraphPad Prism, GraphPad Software, Inc., 2007. www.graphpad.com.

[25] R.H. Kramer, K.G. Bensch, P.M. Davison, M.A. Karasek, Basal lamina formation by cultured microvascular endothelial cells, JCB (J. Cell Biol.) 99 (1984) 692–698, https://doi.org/10.1083/jcb.99.2.692.

[26] E.F. Joy, J.D. Bonn, A.J. Barnard, Photometric determination of trace bromide in alkali metal chlorides, Anal. Chem. 45 (1973) 856–860, https://doi.org/10.1021/ac60328a024.

[27] A.L.P. Chapman, O. Skaff, R. Senthilmohan, A.J. Kettle, M.J. Davies, Hypobromous acid and bromamine production by neutrophils and modulation by superoxide, Biochem. J. 417 (2009) 773–781, https://doi.org/10.1042/BJ20071563.

[28] M. Gazda, D.W. Margerum, Reactions of monochloramine with bromine, tribromide, hypobromous acid and hypobromite: formation of bromochloramines, Inorg. Chem. 33 (1994) 118–123, https://doi.org/10.1021/ic00079a022.

[29] M. Zhou, Z. Diwu, N. Panchuk-Voloshina, R.P. Haugland, A stable nonfluorescent derivative of resorufin for the fluorometric determination of trace hydrogen peroxide: applications in detecting the activity of phagocyte NADPH oxidase and other oxidases, Anal. Biochem. 253 (1997) 162–168, https://doi.org/10.1006/abio.1997.2391.

[30] X. Li, J.A. Imlay, Improved measurements of scant hydrogen peroxide enable experiments that define its threshold of toxicity for Escherichia coli, Free Radic. Biol. Med. 120 (2018) 217–227, https://doi.org/10.1016/j.freeradbiomed.2018.03.025.

[31] D. Dębski, R. Smulik, J. Zielonka, B. Michałowski, M. Jakubowska, K. Dębowska, J. Adamus, A. Marcinek, B. Kalyanaraman, A. Sikora, Mechanism of oxidative conversion of Amplex® Red to resorufin: pulse radiolysis and enzymatic studies, Free Radic. Biol. Med. 95 (2016) 323–332, https://doi.org/10.1016/j.freeradbiomed.2016.03.027.

[32] B. Noszál, D. Visky, M. Kraszni, Population, Acid–Base, and redox properties of *N*-acetylcysteine conformers, J. Med. Chem. 43 (2000) 2176–2182, https://doi.org/10.1021/jm9909600.

[33] F.Q. Schafer, G.R. Buettner, Redox environment of the cell as viewed through the redox state of the glutathione disulfide/glutathione couple, Free Radic. Biol. Med. 30 (2001) 1191–1212.

[34] C. Kerksick, D. Willoughby, The antioxidant role of glutathione and N-Acetyl-Cysteine supplements and exercise-induced oxidative stress, J Int Soc Sports Nutr 2 (2005) 38–44, https://doi.org/10.1186/1550-2783-2-2-38.

[35] R. Kohen, Y. Yamamoto, K.C. Cundy, B.N. Ames, Antioxidant activity of carnosine, homocarnosine, and anserine present in muscle and brain, Proc. Natl. Acad. Sci. USA 85 (1988) 3175–3179, https://doi.org/10.1073/pnas.85.9.3175.

[36] F. Sarrami, L.-J. Yu, A. Karton, Computational design of bio-inspired carnosine-based HOBr antioxidants, J. Comput. Aided Mol. Des. 31 (2017) 905–913, https://doi.org/10.1007/s10822-017-0060-3.

[37] L. Carroll, A. Karton, L. Radom, M.J. Davies, D.I. Pattison, Carnosine and carcinine derivatives rapidly react with hypochlorous acid to form chloramines and dichloramines, Chem. Res. Toxicol. 32 (2019) 513–525, https://doi.org/10.1021/acs.chemrestox.8b00363.

[38] N. Sciaky, J. Presley, C. Smith, K.J.M. Zaal, N. Cole, J.E. Moreira, M. Terasaki, E. Siggia, J. Lippincott-Schwartz, Golgi tubule traffic and the effects of Brefeldin A visualized in living cells, J. Cell Biol. 139 (1997) 1137–1155.

[39] P.T.A. Linders, M. Ioannidis, M. ter Beest, G. van den Bogaart, Fluorescence lifetime imaging of pH along the secretory pathway, ACS Chem. Biol. 17 (2022) 240–251, https://doi.org/10.1021/acschembio.1c00907.

[40] M. Paumann-Page, N.F. Kienzl, J. Motwani, B. Bathish, L.N. Paton, N.J. Magon, B. Sevcnik, P.G. Furtmüller, M.W. Traxlmayr, C. Obinger, M.R. Eccles, C. C. Winterbourn, Peroxidasin protein expression and enzymatic activity in

metastatic melanoma cell lines are associated with invasive potential, Redox Biol. (2021), 102090, https://doi.org/10.1016/j.redox.2021.102090.

[41] Y.-Z. Zheng, L. Liang, High expression of PXDN is associated with poor prognosis and promotes proliferation, invasion as well as migration in ovarian cancer, Ann. Diagn. Pathol. 34 (2018) 161–165, https://doi.org/10.1016/j.anndiagpath.2018.03.002.

[42] A. Jayachandran, P. Prithviraj, P.-H. Lo, M. Walkiewicz, M. Anaka, B.L. Woods, B. Tan, A. Behren, J. Cebon, S.J. McKeown, Identifying and targeting determinants of melanoma cellular invasion, Oncotarget 7 (2016) 41186–41202, https://doi.org/10.18632/oncotarget.9227.

[43] M. Soudi, M. Paumann-Page, C. Delporte, K.F. Pirker, M. Bellei, E. Edenhofer, G. Stadlmayr, G. Battistuzzi, K.Z. Boudjeltia, P.G. Furtmüller, P.V. Antwerpen, C. Obinger, Multidomain human peroxidasin 1 is a highly glycosylated and stable homotrimeric high spin ferric peroxidase, J. Biol. Chem. 290 (2015) 10876–10890, https://doi.org/10.1074/jbc.M114.632273.

[44] B. Sevcnikar, M. Paumann-Page, S. Hofbauer, V. Pfanzagl, P.G. Furtmüller, C. Obinger, Reaction of human peroxidasin 1 compound I and compound II with one-electron donors, Arch. Biochem. Biophys. 681 (2020), https://doi.org/10.1016/j.abb.2020.108267, 108267.

[45] J. Flemmig, J. Zschaler, J. Remmler, J. Arnhold, The fluorescein-derived dye aminophenyl fluorescein is a suitable tool to detect hypobromous acid (HOBr)-producing activity in eosinophils, J. Biol. Chem. 287 (2012) 27913–27923, https://doi.org/10.1074/jbc.M112.364299.

[46] J. Flemmig, J. Remmler, J. Zschaler, J. Arnhold, Detection of the halogenating activity of heme peroxidases in leukocytes by aminophenyl fluorescein, Free Radic. Res. 49 (2015) 768–776, https://doi.org/10.3109/10715762.2014.999676.